Mechanistic studies of oxygen reduction on Fe-PEI derived non-PGM electrocatalysts

Alexey Serov [a,1], Urszula Tylus [b,1], Kateryna Artyushkova [a], Sanjeev Mukerjee [b], Plamen Atanassov [a,*]

[a] Department of Chemical and Nuclear Engineering, 1 University of New Mexico, University of New Mexico, Albuquerque, NM 87131, USA
[b] Department of Chemistry and Chemical Technology, Northeastern University, Boston, MA 02115, USA

ARTICLE INFO

ABSTRACT

Mechanistic studies of oxygen reduction reaction (ORR) on electrocatalysts derived from the pyrolysis of iron salts and polyethyleneimine (PEI) were performed in acidic and alkaline media. The prepared materials have been characterized by scanning electron microscopy (SEM), X-ray photoelectron spectroscopy (XPS), Brunauer–Emmett–Teller (BET) surface area analysis, and rotating ring-disk electrode (RRDE) methods. Systematic studies of catalyst loading on working electrode allowed establishing a working range suitable for mechanistic studies. It was found that the overall mechanism of ORR in acid electrolyte is not identical with that in alkaline media indicating complex interplay. The dependence of electron transfer numbers on catalyst loading indicates $2 \times 2e^-$ mechanism. The analysis of the Tafel plots corresponding to electrode polarizations have demonstrated difference of the reaction rate limiting steps in alkaline and acid media.

© 2013 Elsevier B.V. All rights reserved.

1. Introduction

The substitution of platinum, platinum group metals (PGM) and their alloys from membrane electrode assembly (MEA) will substantially reduce overall cost and market acceptance of fuel cell devices, bringing them closer to introduction into commonplace. To achieve this goal significant investment in development of non-platinum and non-PGM catalysts for fuel oxidation [1] and oxygen reduction [2] were undertaken. The main focus in non-PGM electrocatalysts is preparation of highly active and durable materials for cathode applications in polymer electrolyte membrane fuel cells (PEMFC).

Palladium [3–5] or Ru compounds [6–10] despite their high activity in ORR can be only temporary solution for platinum substitution due to their high price, low abundance, and durability issues. At the moment most active and inexpensive cathode catalysts mainly consist of transition metal, nitrogen, and carbon and are abbreviated in literature as M–N–C. Traditionally metal macrocycles such as, porphyrins and phtalocianines, compounds with transition metal coordinated by nitrogen have been pyrolyzed in order to produce highly active M–N–C materials [14–23]. The last

decade saw the rise of an alternative way of making catalyst of the same class by heat treatments of combination of transition metal precursor and source of carbon and nitrogen [24–31].

A major design point of non-PGM catalysts is facilitating oxygen reduction reaction by direct 4e− mechanism. The determination of ORR pathways is mainly performed by rotation ring disk electrode (RRDE) technique. The method allows obtaining such important parameters as hydrogen peroxide yield, number of electrons participating in oxygen reduction reaction, rate-limiting steps etc. However, it should be taking into account that some of these parameters can be greatly affected by amount of catalyst deposited onto the surface of working electrode. In case of highly porous catalyst or material with high surface area hydrogen peroxide, although formed, can undergo further conversion to water electrochemically or to be decomposed to water and oxygen in a non-electrochemical reaction of disproportionation. It this case the overall number of electrons collected will be 4, demonstrating "4e− stoichiometry" that could be misinterpreted as "4e− mechanism". Recently at UNM we synthesized a family of non-platinum catalysts and performed mechanistic studies on several of them. These M–N–C catalysts were synthesized by sacrificial support method (SSM), which was developed at UNM [32–41].

In the present work electrocatalysts derived from pyrolysis of iron salt and a polymer carbon-nitrogen precursor, polyethyleneimine (Fe-PEI) were synthesized at NEU by conducting the pyrolysis on carbon black support ("traditional method"). The
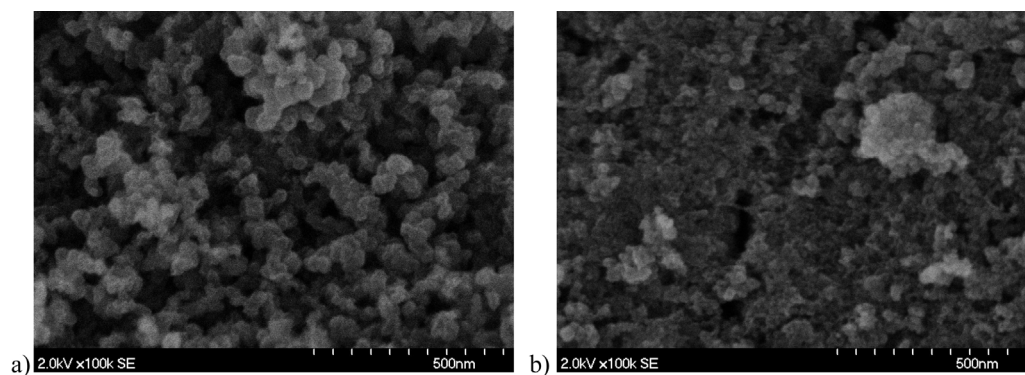
Fig. 1. SEM images for Fe-PEI-1 (a) and Fe-PEI-2 (b) catalysts.

cross-lab mechanistic studies of oxygen reduction reaction were performed in acidic and alkaline media by RRDE method. Influence of catalyst loading on hydrogen peroxide yield was systematically studied. Koutecky–Levich and Tafel analysis was used to determine number of electrons and rate limiting step.

2. Materials and methods

2.1. Catalysts preparation

Both, the Fe-PEI-1 and Fe-PEI-2 catalysts were synthesized from branched polyethyleneimine (50–100 kMW) and ferric chloride as nitrogen and metal source, respectively. Initially, 10 wt.% solution of the metal salt was added drop wise to 10 wt.% solution of the PEI while stirring. In case of the FePEI-1, the mixture was left stirring over 12 h (Fe-PEI-1) to allow full complexation, while the Fe-PEI-2 was stirred for 15 min, followed by evaporation of solvent in vacuum oven at 80 °C over period of 12 h. The metal-polymer network was then supported on high surface area carbon black (Ketjen Black 600 JD) at 1:1 complex to carbon ratio using dry impregnation method. The supported polymer-carbon hybrid materials were pyrolyzed at $T = 850$ °C in argon atmosphere. In order to increase ORR activity the second heat treatment was performed for both materials at the same conditions as a first pyrolysis: $T = 850$ °C in argon atmosphere.

2.2. Ring disk electrode

Electrochemical analysis for synthesized catalysts was performed using the Pine Instrument Company electrochemical analysis system. The rotational speeds were: 400, 900, 1200 and 1600 rpm, with a scan rate of 10 mV s^{-1}. The electrolytes were 0.5 M H_2SO_4 and 1 M KOH saturated in O_2 at room temperature. A platinum wire counter electrode, Ag/AgCl reference electrode in case of acidic media and Hg/HgO in case of alkaline media were used.

Working electrodes were prepared by mixing 5 mg of the Fe-PEI electrocatalyst with 850 μL of isopropyl alcohol, and 150 μL of Nafion® (0.5 wt.%, DuPont). The mixture was sonicated before 5, 10, 20 and 30 μL was applied onto a glassy carbon disk with a sectional area of 0.2474 cm^2. The loadings of catalyst on the electrode were: 0.1, 0.2, 04 and 0.6 mg cm^{-2}.

2.3. Characterization

Scanning electron microscopy was performed on a Hitachi S-800 instrument.

XPS spectra were acquired on a Kratos Axis DLD Ultra X-ray photoelectron spectrometer using an Al Kα source monochromatic operating at 150 W with no charge compensation. The base pressure was about 2×10^{-10} Torr, and operating pressure was around 2×10^{-9} Torr. Survey and high-resolution spectra were acquired at pass energies of 80 and 20 eV respectively. Acquisition time for
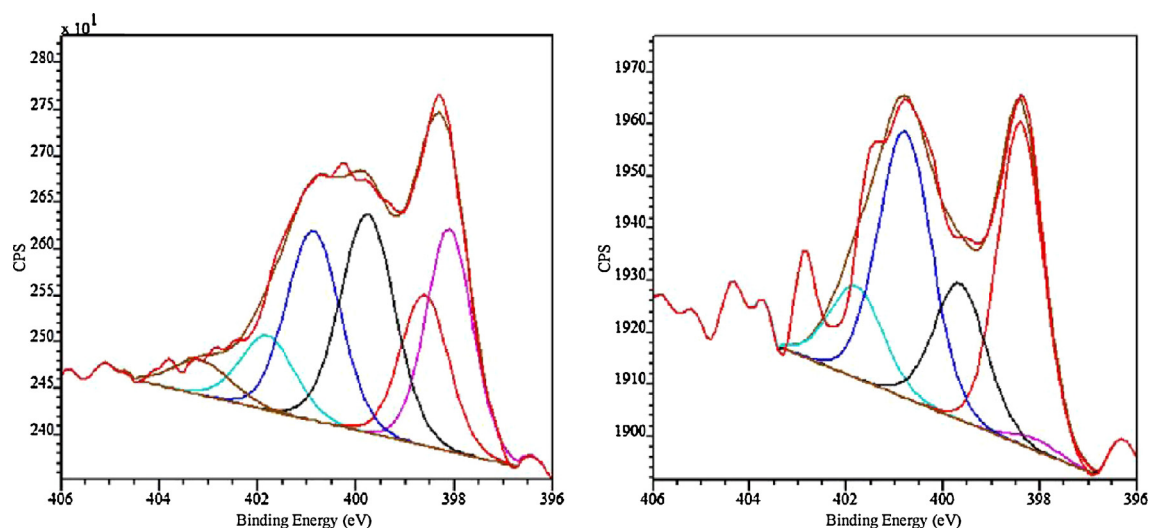

Fig. 2. High resolution N1s spectra for (a) pyrolyzed Fe-PEI-2 (b) Fe-PEI-1 pyrolyzed in argon atmosphere.
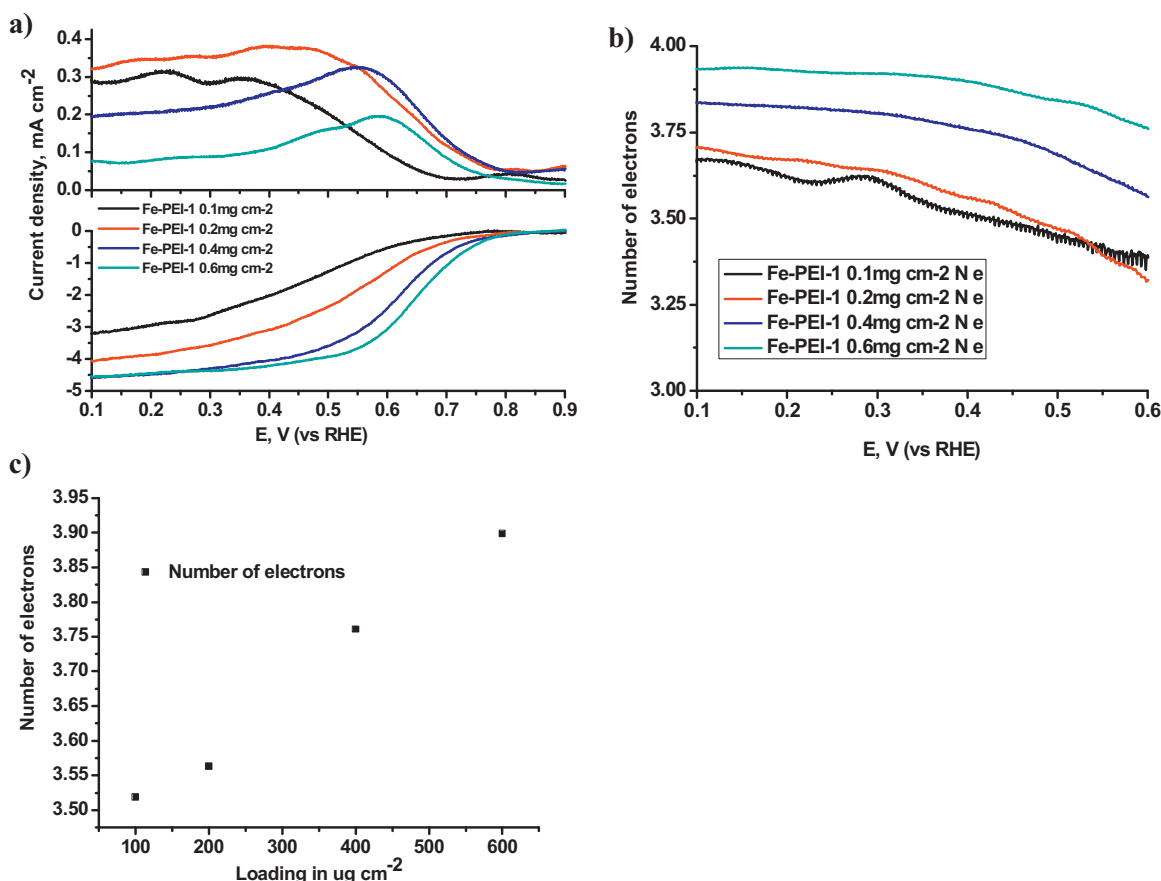
Fig. 3. Electrochemical data for Fe-PEI-1 catalyst with different loadings: (a) ORR performance, (b) number of electrons and (c) dependence of N_e on loading for: $l = 0.1$ mg cm^{-2} (—), $l = 0.2$ mg cm^{-2} (— —), $l = 0.4$ mg cm^{-2} (·· ·) and $l = 0.6$ mg cm^{-2} (— · —). Conditions: 0.5 M H$_2$SO$_4$ saturated with O$_2$, 1200 rpm, 5 mV s^{-1}, catalyst loading 0.6 mg cm^{-2}.

survey spectra was 2 min, for C1s and O1s spectra −5 min, for N1s and Fe 2p −30 min. Data analysis and quantification were performed using CasaXPS software. A linear background subtraction was used for quantification of C1s, O1s and N1s spectra, while a Shirley background was applied to Fe 2p spectra. Sensitivity factors provided by the manufacturer were utilized. A 70% Gaussian/30% Lorentzian line shape was utilized in the curve-fit of N1s.

3. Results and discussion

It was observed by SEM that Fe-PEI-1 and Fe-PEI-2 have different morphology (Fig. 1). While Fe-PEI-1 has uniform and well dispersed particles, Fe-PEI-2 is substantially agglomerated. The surface area of the Fe-PEI-1 (estimated with 5 points Brunauer–Emmett–Teller method) was found to be more than two times higher compared to SA of Fe-PEI-2 (870 vs. 430 m^2/g, respectively). Such a difference in morphology and surface area can be explained by variations in synthesis due to differences in complexation efficiency through various rates of metal salt addition into the polymer, insufficient stirring and shorter reaction time in case of Fe-PEI-2. As a result, part the iron precursor was poorly dispersed, resulting in inhomogeneous distribution of polymer-carbon-iron material.

XPS analysis revealed that materials mainly consist of carbon with several atomic percents of nitrogen and oxygen. Fe-PEI-1 sample has 1.6 % of N while Fe-PEI-2 has only 0.3 % of N. Fig. 2 shows N1s high resolution spectra representative of good and bad electrocatalysts. Six peaks of the same full width half maximum (FWHM), determined at the same acquisition setting for polypridine to be

1.2 eV, was used to curve fit N1s spectra. These six peaks correspond to six types of nitrogen, such as nitrile (398 eV), pyridinic (398.6 eV), N$_x$-Fe (399.6 eV), pyrrolic N (400.7 eV), quaternary (401.8 eV) and graphitic (403 eV) nitrogens. The Fe-PEI-1 and Fe-PEI-2 catalysts have obviously different distribution of N species Fig. 2. Relative amount of N$_x$-Fe centers is higher for Fe-PEI-1 compared to Fe-PEI-2 sample. The amount of pyrrolic N, which was shown to be responsible for the first 2e$^-$ step of O$_2$ to H$_2$O$_2$ reduction, in the Fe-PEI-2 sample is significantly larger than in Fe-PEI-1 sample.

The dependence of ORR activity on catalyst loading is shown on Fig. 3a. As the Fig. 3a clearly indicates the increase in catalyst loading results in increasing both limiting current and E$_{1/2}$. Consistently, the slope of the kinetic region of ORR polarization curves persistently increases with the loading until it becomes well pronounced. This suggest that determination of catalytic activity of non-PGM catalyst with lower concentration of active centers needs to be performed at the higher loading, between 0.4–0.6 mg cm^{-2}. Overall number of electrons can be calculated from RRDE data by Eq. (1).

$$n = \frac{4I_D}{\left(\frac{I_D + I_R}{N}\right)} \tag{1}$$

where n is number of electrons, I_R, I_D and N are the ring current, disk current and ring collection efficiency (0.37), respectively. It should be noted, that the background current observed in the ring response at potentials above the reaction onset (above ∼0.8 V) was removed before analysis by its subtraction from the ring signal throughout the whole range of the applied potential range.
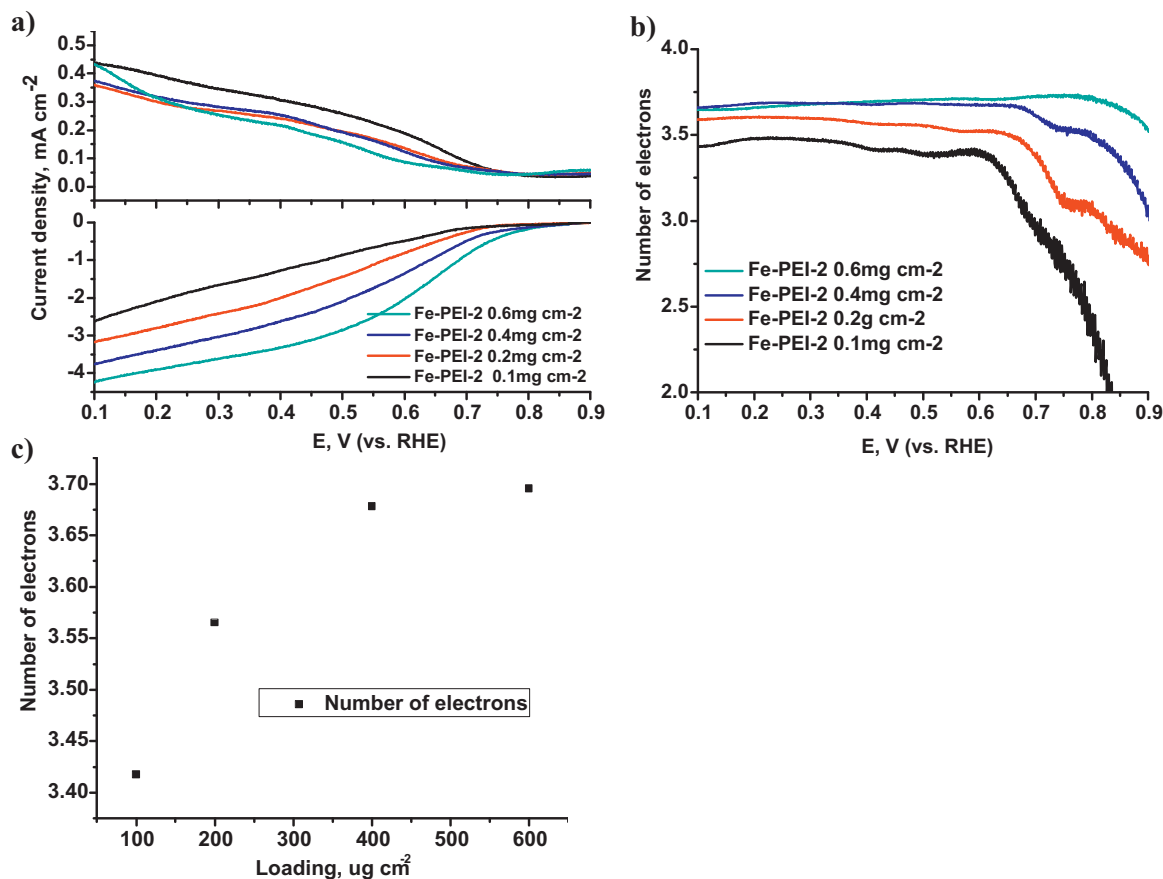
Fig. 4. Electrochemical data for Fe-PEI-2 catalysts with different loadings: (a) ORR performance, (b) number of electrons and (c) dependence of N_e on loading for: l = 0.1 mg cm^{-2} (——), l = 0.2 mg cm^{-2} (— —), l = 0.4 mg cm^{-2} (· · ·) and l = 0.6 mg cm^{-2} (— · —). Conditions: 0.5 M H_2SO_4 saturated with O_2, 1200 rpm, 5 mV s^{-1}, catalyst loading 0.6 mg cm^{-2}.

It was found that with increase of loading the number of electrons increases as well, reaching about 4e$^-$ (Fig. 4b,c). Such dependence indicates indirect 2×2 electron mechanism, where oxygen is first reduced to H_2O_2 followed by further electroreduction to H_2O. In order to determine realistic number of electrons the lowest loading of catalysts is recommended to be used. The RRDE data of the Fe-PEI-2 catalyst in acid is shown in Fig. 5. It was observed that the catalyst has lower activity (by $E_{1/2}$) compared to Fe-PEI-1. This can be explained by limited accessibility of active sites to oxygen due to particles agglomeration resulted in lower surface area. Further, the poor performance of the Fe-PEI-2 may be a result of lower overall density the N_x-Fe centers as earlier observed by XPS. On the other hand, the similar behavior of catalyst loading vs. Number of electron as in case of Fe-PEI-1 can be indication of similarity in ORR mechanism for both catalysts.

The same RRDE experiments that were performed in acid were also conducted in alkaline (Figs. 6 and 7). It was found that at pH 14 both catalysts have substantially higher performance towards oxygen reduction. The $E_{1/2}$ values observed for both non-PGM catalysts were close to the $E_{1/2}$ values of Pt/C catalyst [42]. However, the dependence of the electrons number on catalyst loading revealed that in case of Fe-PEI-2 mechanism is close to pure 2e$^-$ O_2 electroreduction.

The determination of mechanism based on analysis of hydrogen peroxide has its limitations due to detection of H_2O_2 on platinum ring. It is well known that H_2O_2 can be chemically decomposed on multiple surface moieties, especially in presence of metal. Taking this fact into account we performed in-depth analysis of kinetic parameters based on Koutecky–Levich (KL) and Tafel approaches.

The RDE experiments at different rotation rates were performed for Fe-PEI-1 and Fe-PEI-2 catalysts in acid and alkaline media. Using Koutecky–Levich equation (Eq. (2)) and plotting $|j_d|^{-1}$ against $\omega^{-1/2}$, allows us to extrapolate the j_k and n in a system where all of the other values are known

$$\frac{1}{j_d} = \frac{1}{j_k} + \frac{1}{0.62 n F C_{O_2} D_{O_2}^{2/3} v^{-1/6} \omega^{1/2} A} \tag{2}$$

where j_k is the electrode potential dependent kinetic current density of the ORR, n is the average number of electrons transferred per catalytic event (the theoretical maximum is 4), F is the Faraday's constant (96,487 C mol^{-1}), C_{O_2} is the concentration of molecular oxygen in the electrolyte (1.117 E^{-6} mol mL^{-1} in acid and 8.40E-07 mol mL^{-1} in alkaline) D_{O_2} is the O_2 diffusion coefficient in aqueous media (1.9 E^{-5} cm^2 s^{-1}), and v is the kinetic viscosity of the electrolyte (0.01000 cm^2 s^{-1} for acid, and 0.01073 cm^2 s^{-1} for alkaline), ω is the angular momentum in rads s^{-1}, and A is the sectional area of the electrode.

The KL plots for Fe-PEI-1 in acid (Fig. 8a) and in alkaline media (Fig. 8b) have a similar slope and number of electrons extracted from Eq. (2) is very similar and close to 4e$^-$. Despite the fact that KL plots for Fe-PEI-2 were similar in acid (Fig. 9a) and alkaline (Fig. 9b) as well, the number of electrons was found to be close to 3e$^-$.

The Tafel method was used to obtain the kinetic parameters of the oxygen reduction of Fe-PEI catalysts. The kinetic part of ORR plat with j_d independent of rotational rate, down to 0.7 V in acid,
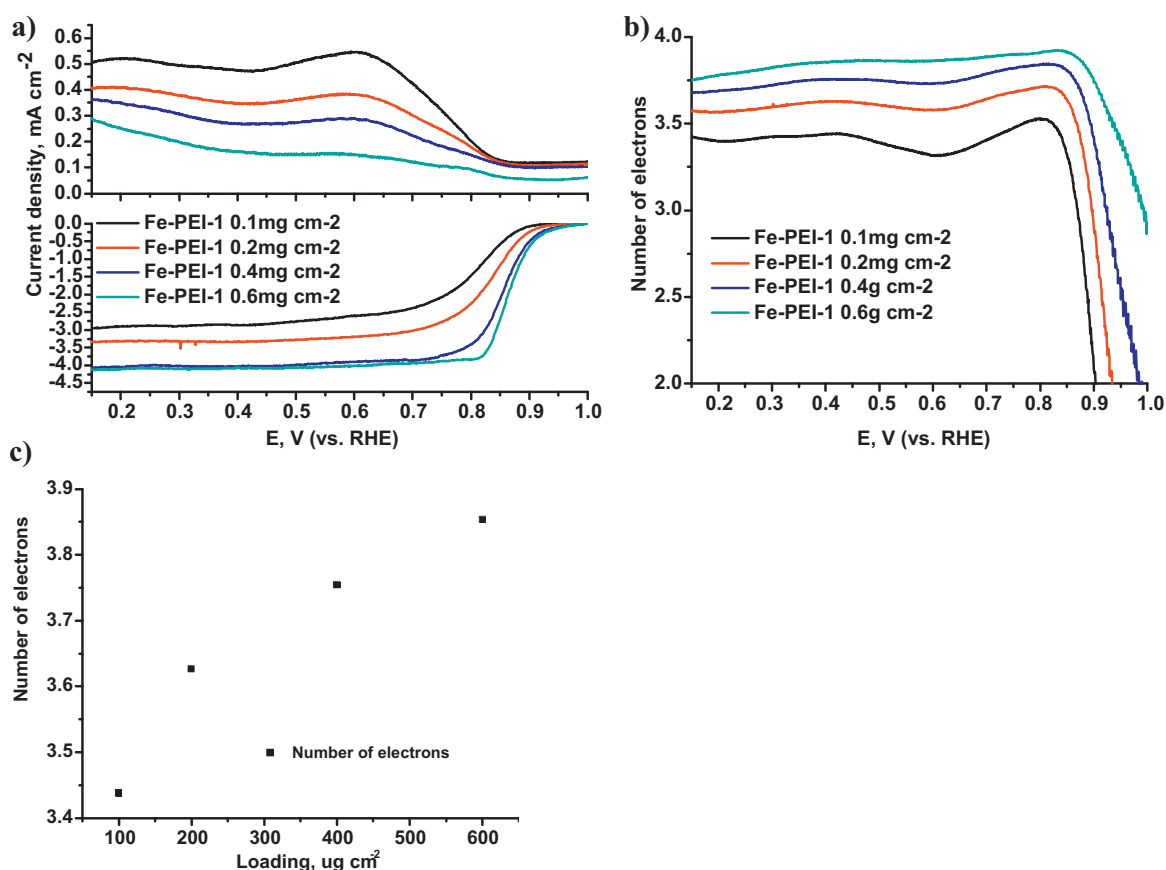
Fig. 5. Electrochemical data for Fe-PEI-1 catalysts with different loadings: (a) ORR performance, (b) number of electrons and (c) dependence of N_e on loading for: l = 0.1 mg cm^{-2} (——), l = 0.2 mg cm^{-2} (— —), l = 0.4 mg cm^{-2} (· · ·) and l = 0.6 mg cm^{-2} (— · —). Conditions: 1 M KOH saturated with O_2, 1200 rpm, 5 mV s^{-1}, catalyst loading 0.6 mg cm^{-2}.

Table 1
Kinetic current densities and exchange current densities for the electrocatalysts in this study in both acid and alkaline electrolytes and at four different loadings at the RRDE experiment.

	Loading (mg/cm^{-2})	n		j_k (mA cm^{-2})		α		j^0 (mA cm^{-2})		k_e (cm s^{-1})	
		Good	Bad	Good	Bad	Good	Bad	Good	Bad	Good	Bad
0.5 M H$_2$SO$_4$	100	2.9	NA	0.26	0.09	0.75	0.31	1.68E-08	3.85E-04	1.58E-10	3.62E-06
0.70 V	200	3.4	NA	0.25	0.11	0.84	0.35	1.70E-09	1.70E-04	1.61E-11	1.60E-06
	400	3.9	3.3	0.22	0.10	0.85	0.33	5.78E-09	4.11E-04	5.45E-11	3.87E-06
	600	4.1	3.3	0.24	0.10	1.00	0.32	3.80E-10	6.69E-04	3.58E-12	6.31E-06
1 M NaOH	100	3.1	2.3	0.31	0.37	0.95	0.85	2.67E-06	7.25E-06	3.29E-08	8.94E-08
0.9 V	200	3.3	2.5	0.25	0.25	0.83	0.63	2.01E-05	1.98E-04	2.48E-07	2.45E-06
	400	3.8	3	0.27	0.29	1.03	0.85	2.04E-06	6.98E-06	2.52E-08	8.62E-08
	600	4.4	3.2	0.26	0.22	1.10	0.70	8.14E-07	1.26E-04	1.00E-08	1.55E-06

NA, not available.

Table 2
Tafel slopes and intercepts of the polarization curves for ORR conducted under RRDE conditions with the electrocatalysts in this study in both acid and alkaline electrolytes and at four different loadings.

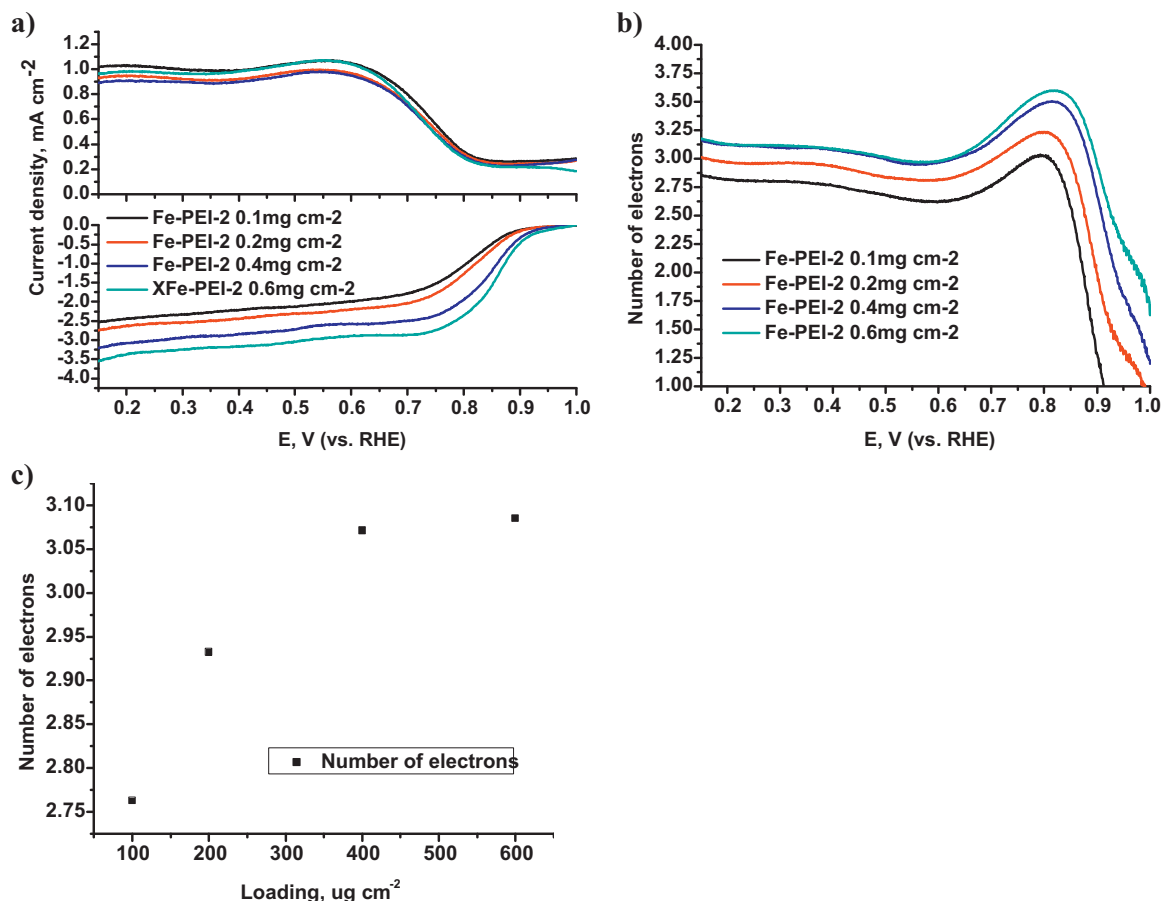|	Loading (mg/cm^{-2})	Tafel slope [mV/dec]		R^2 fit		Y_{int} (V)	
		Fe-PEI-1	Fe-PEI-2	Fe-PEI-1	Fe-PEI-2	Fe-PEI-1	Fe-PEI-2
0.5 M H$_2$SO$_4$	100	79	178	0.992	0.987	0.84	0.98
	200	70	159	0.972	0.997	0.85	1.02
	400	69	169	0.937	0.999	0.9	1.07
	600	59	176	0.985	0.999	0.91	1.17
1 M KOH	100	62	69	0.996	0.983	0.98	1.1
	200	71	93	0.998	0.99	1.01	1.05
	400	57	69	0.999	0.983	1.01	1.1
	600	52	84	0.998	0.998	1.03	1.14

Fig. 6. Electrochemical data for Fe-PEI-2catalysts with different loadings: (a) ORR performance, (b) number of electrons and (c) dependence of N_e on loading for: l = 0.1 mg cm^{-2} (——), l = 0.2 mg cm^{-2} (— —), l = 0.4 mg cm^{-2} (· · ·) and l = 0.6 mg cm^{-2} (— · —). Conditions: 1 M KOH saturated with O_2, 1200 rpm, 5 mV s^{-1}, catalyst loading 0.6 mg cm^{-2}.

and 0.90 V in alkaline was used for analysis. The kinetic current density can be described using the expression (Eq. (3)):

$$E = E^0 + \frac{2.30RT}{\alpha\eta_\alpha F} \log(j^0) - \frac{2.30RT}{\alpha\eta_\alpha F} \log(j_d) \tag{3}$$

where α is the symmetry coefficient for electron transfer in the rate-determining step (RDS), which is postulated to be adsorption of molecular oxygen on the active center of the catalyst and formation of peroxide moiety with participation of 1

electron (Catalyst + O_2 + H + (aq) + e$^-$ = Catalyst-OOH), n_α is the number of electrons transferred in the RDS, and as consequence of the above postulate is presumed to be 1, E is the electrode potential as applied, E^0 is the thermodynamic electrode potential of the ORR (1.23 V vs. RHE), R is the universal gas constant (8.314 J mol^{-1} K^{-1}), T is the temperature in terms of K (298 K), and F is the Faraday constant (96,487 C mol^{-1}). The plot of E as a function of $\log(j_d)$ (Fig. 10) gives information about the kinetic parameters of the ORR that can be derived from the line equation for specific regions of
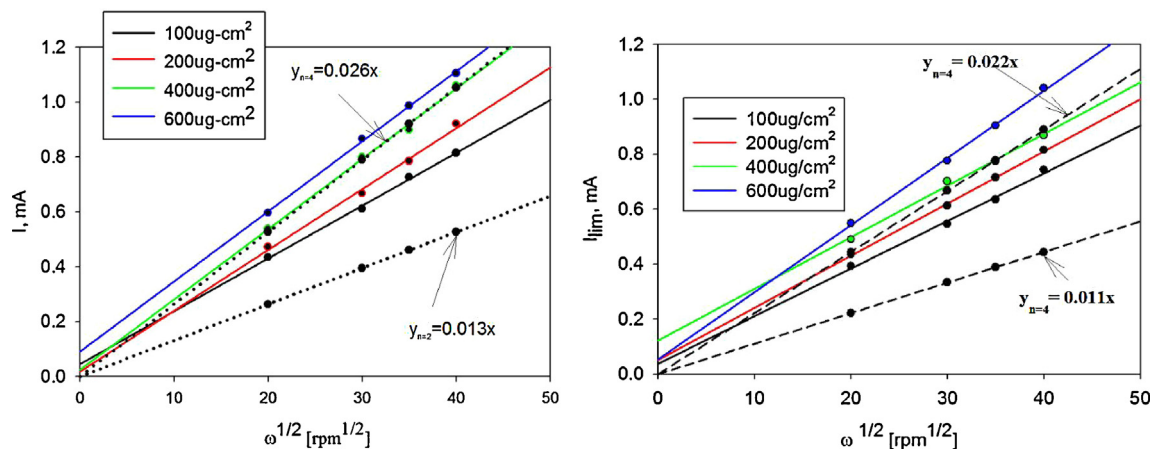

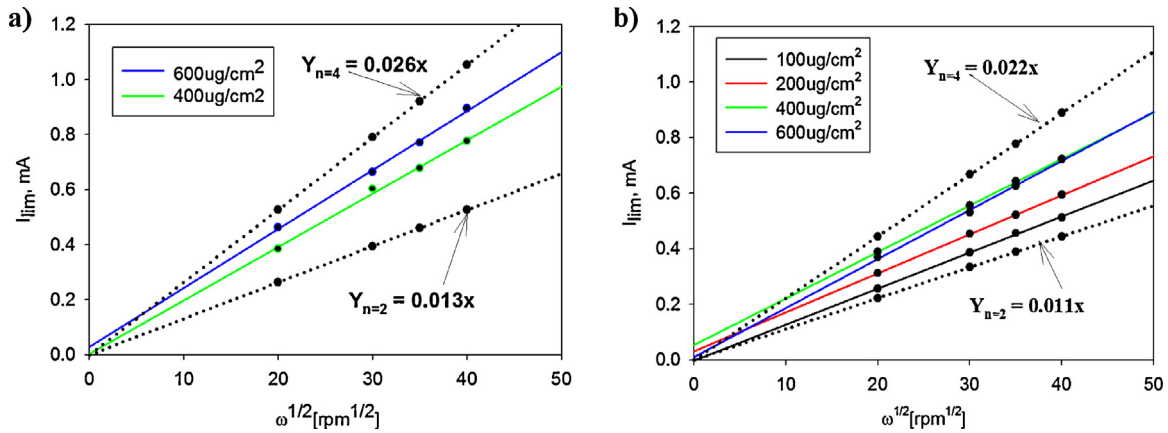**Fig. 7.** KL plot on Fe-PEI catalysts (a) Fe-PEI-1 in acid and (b) Fe-PEI-1 in alkaline.

Fig. 8. KL plot on Fe-PEI catalysts (a) Fe-PEI-2 in acid and (b) Fe-PEI-2 in alkaline. Note: No limited current was obtained in the low loadings of the catalyst in acid.
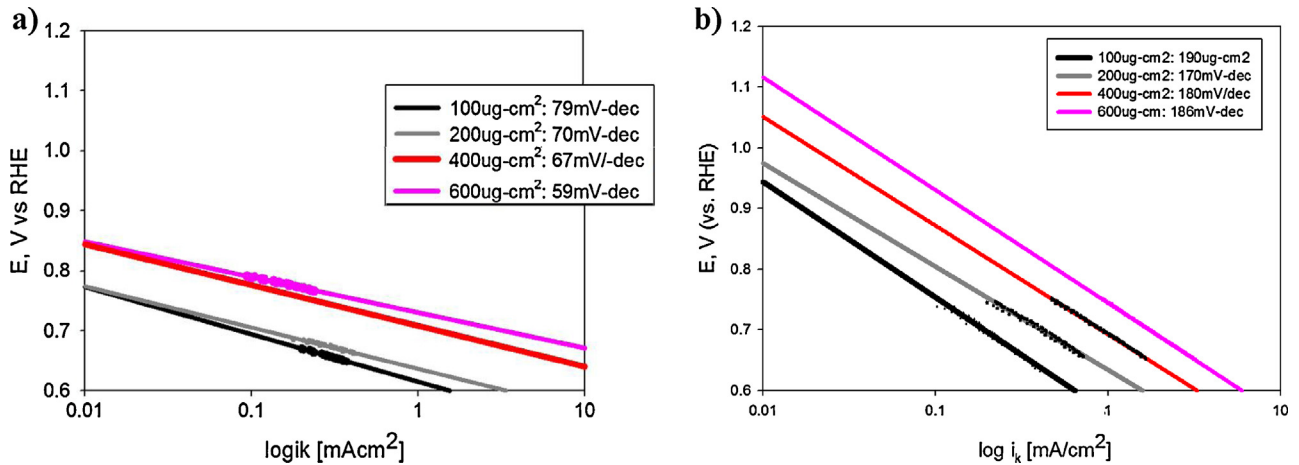

Fig. 9. Tafel plot for (a) Fe-PEI-1 catalyst in acid and (b) Fe-PEI-2 catalyst in acid.

the plot. The Tafel slope ($=2.303RT \cdot \alpha^{-1} n_\alpha^{-1} F^{-1}$) and the intercept ($=E^0 + (2.303RT \cdot \alpha^{-1} n_\alpha^{-1} F^{-1}) \log(j_d)$) allow for the values of α and j^0, which is the exchange current density, to be calculated when all other values are known. The corresponding values for j^0 for each loading in both media are listed in Table 1, along with the kinetic rate constant (k_e) for the RDS, while Table 2 lists the suitability of the fit of the line in the region of interest, as well as the slope and

y intercept, for the Tafel plots from which this information was obtained. The relationship between j^0 and k_e is defined as

$$j^0 = nFk_eC_{O_2} \tag{4}$$

where the n is the Koutecky–Levich determined number of transferred electrons.
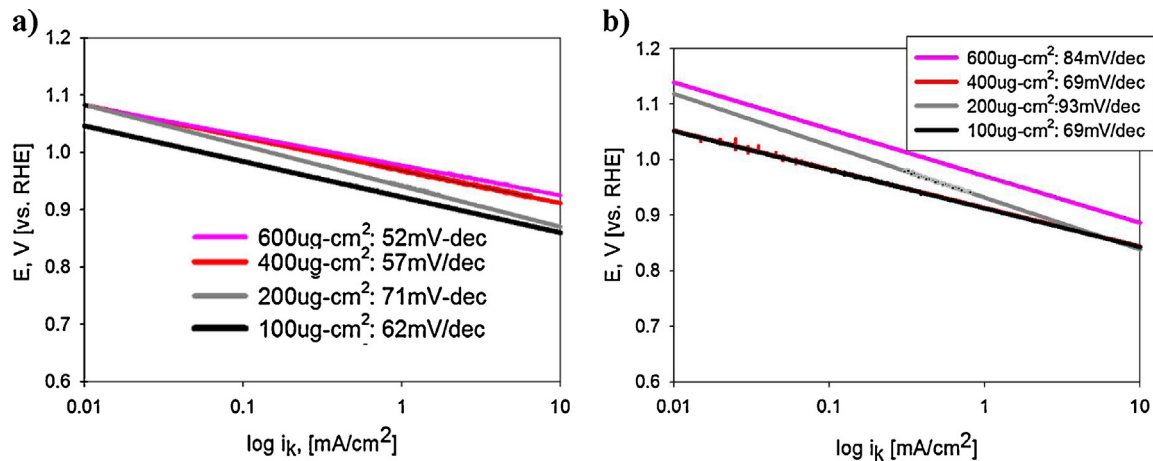

Fig. 10. Tafel plot for (a) Fe-PEI-1 catalyst in alkaline and (b) Fe-PEI-2 catalyst in alkaline.

The Tafel plots for Fe-PEI-1 in both acid and alkaline media have similar slope with close to 60 mV per decade values (Fig. 10a and b). The kinetic currents j_k were found to be close 0.25 mA cm^{-2} in both electrolytes. However, Fe-PEI-2 had a completely different slopes and kinetic parameters in acid compared to alkaline. A slope of ~160 mV per decade in acidic electrolyte that can be interpreted as slow kinetics in oxygen reduction. Comparison of Tafel slopes for Fe-PEI-1 and Fe-PEI-2 in alkaline media revealed similar rate of reaction (Tables 1 and 2). An explanation of this observation can be in the morphology effect on "masking" the true kinetic behavior. This can be correlated with the agglomerated morphology of the catalyst.

4. Conclusions

Non-PGM catalysts for oxygen reduction based on pyrolyzed Fe-PEI material were synthesized and fully characterized. The materials have different morphology as it was determined by SEM as well substantial different surface chemical species, as it was shown by XPS.

Detailed mechanistic studies revealed that Fe-PEI-2 catalyst has a different mechanism of oxygen reduction in acid compared to alkaline media, while Fe-PEI-1 has the same. Analysis of number of electrons participating in ORR by H$_2$O$_2$ flux and Koutecky–Levich methods indicates indirect $2 \times 2e^-$ mechanism.

The experiments on correlation of surface chemistry with performance are currently ongoing.

Acknowledgement

References

[1] F. Jaouen, E. Proietti, M. Lefèvre, R. Chenitz, J.-P. Dodelet, G. Wu, H.T. Chung, C.M. Johnston, P. Zelenay, Energy Environ. Sci. 4 (2011) 114–130.
[2] A. Serov, C. Kwak, Appl. Catal., B 91 (2009) 1–10.
[3] E. Antolini, Energy Environ. Sci. 2 (2009) 915–931.
[4] A. Serov, T. Nedoseykina, O. Shvachko, C. Kwak, J. Power Sources 195 (2010) 175–180.
[5] A.A. Serov, S.-Y. Cho, S. Han, M. Min, G. Chai, K.H. Nam, C. Kwak, Electrochem. Commun. 9 (2007) 2041–2044.
[6] D.T. Whipple, R.S. Jayashree, D. Egas, N. Alonso-Vante, P.J.A. Kenis, Electrochim. Acta 54 (2009) 4384–4388.
[7] Y. Feng1, A. Gago, L. Timperman, N. Alonso-Vante, Electrochim. Acta 56 (2011) 1009–1022.
[8] A.A. Serov, M. Min, G. Chai, S. Han, S. Kang, C. Kwak, J. Power Sources 175 (2008) 175–182.
[9] V. Le Rhun, E. Garnier, S. Pronier, N. Alonso-Vante, Electrochem. Commun. 2 (2000) 475–479.
[10] A.A. Serov, C. Kwak, Catal. Commun. 10 (2009) 1551–1554.
[14] T.S. Olson, S. Pylyplenko, P. Atanassov, J. Phys. Chem. C 114 (2010) 5049–5059.
[15] R. Jasinski, Nature 201 (1964) 1212.
[16] H. Jahnke, M. Schönborn, G. Zimmermann, Top. Curr. Chem. 61 (1976) 133.
[17] V.S. Bagotzky, M.R. Tarasevich, K.A. Radyushkina, O.E. Levina, S.I. Andrusyova, J. Power Sources 2 (1977) 233.
[18] S. Gupta, D. Tryk, I. Bae, W. Aldred, E. Yeager, J. Appl. Electrochem. 19 (1989) 19.
[19] U.I. Koslowski, I. Abs-Wurmbach, S. Fiechter, P. Bogdanoff, J. Phys. Chem. C 112 (2008) 15356.
[20] J. Maruyama, J. Okamura, K. Miyazaki, Y. Uchimoto, I. Abe, J. Phys. Chem. C 112 (2008) 2784.
[21] T.S. Olson, K. Chapman, P. Atanassov, J. Power Sources 183 (2008) 557.
[22] J.M. Ziegelbauer, T.S. Olson, S. Pylypenko, F. Alamgir, C. Jaye, P. Atanassov, S. Mukerjee, J. Phys. Chem. C 112 (2008) 8839.
[23] A.A. Serov, M. Min, G. Chai, S. Han, S.J. Seo, Y. Park, H. Kim, C. Kwak, J. Appl. Electrochem. 39 (2009) 1509.
[24] J.I. Ozaki, S.I. Tanifuji, A. Furuichi, K. Yabutsuka, Electrochim. Acta 55 (2010) 1864.
[25] T.S. Olson, S. Pylypenko, J.E. Fulghum, P. Atanassov, J. Electrochem. Soc. 157 (2010) B54.
[26] Y. Nabae, S. Moriya, K. Matsubayashi, S.M. Lyth, M. Malon, L. Wu, N.M. Islam, Y. Koshigoe, S. Kuroki, M.A. Kakimoto, S. Myata, J.I. Ozaki, Carbon 48 (2010) 2613.
[27] I. Herrmann, U.I. Kramm, S. Fiechter, V. Brüser, H. Kersten, P. Bogdanoff, Plasma Process. Polym. 7 (2010) 515.
[28] J.D. Wiggins-Camacho, K.J. Stevenson, J. Phys. Chem. C 113 (2009) 19082.
[29] K. Prehn, A. Warburg, T. Schilling, M. Bron, K. Schulte, Compos. Sci. Technol. 69 (2009) 1570.
[30] Z. Chen, D. Higgins, H. Tao, R.S. Hsu, Z. Chen, J. Phys. Chem. C 113 (2009) 21008.
[31] G. Wu, Z. Chen, K. Artyushkova, F.H. Garzon, P. Zelenay, ECS Trans. 16 (2008) 159.
[32] S. Pylypenko, S. Mukherjee, T.S. Olson, P. Atanassov, Electrochim. Acta 53 (2008) 7875–7883.
[33] M.H. Robson, A. Serov, K. Artyushkova, P. Atanassov, Electrochim. Acta 90 (2013) 656–665.
[34] S. Brocato, A. Serov, P. Atanassov, Electrochim. Acta 87 (2013) 361–365.
[35] A. Serov, M.H. Robson, K. Artyushkova, P. Atanassov, Appl. Catal., B 127 (2012) 300–306.
[36] A. Serov, M.H. Robson, M. Smolnik, P. Atanassov, Electrochim. Acta 80 (2012) 213–218.
[37] A. Serov, U. Martinez, A. Falase, P. Atanassov, Electrochem. Commun. 22 (2012) 193–196.
[38] A. Serov, M.H. Robson, B. Halevi, K. Artyushkova, P. Atanassov, Electrochem. Commun. 22 (2012) 53–56.
[39] A. Falase, M. Main, K. Garcia, A. Serov, C. Lau, P. Atanassov, Electrochim. Acta 66 (2012) 295–301.
[40] A. Serov, U. Martinez, P. Atanassov, Electrochem. Commun. 34 (2013) 185–188.
[41] A. Serov, M.H. Robson, M. Smolnik, P. Atanassov, Electrochim. Acta 109 (2013) 433–439.
[42] H.T. Chung, J.H. Won, P. Zelenay, Nat. Commun. 4 (2013) 1922, DOI 10.1038/ncomms2944.